URSI-B EMTS 2025, Bologna, 23–27 June

A Scalable open-source electromagnetics model for Wireless power transfer and Space-Based Solar Power

Timothy Pelham*(1), Thomas Fearon(1)
(1) Communications, Systems & Networks Laboratory, University of Bristol, UK

Abstract

Space-based solar power has been proposed as early as the 1960s as a source of reliable and clean energy. Due to reductions in the cost of orbital access it has received renewed interest in recent years. A practical challenge to the deployment of these systems is the requirement for ultra-large scale antenna arrays for wireless power transfer at scale, with proposed GW scale systems with antenna array diameters on the order of 2km, with billions of antenna elements. In this paper a development of the Rayleigh-Sommerfeld Diffraction Integral is introduced together with CUDA accelerated ray tracing for flexible modelling. A simplified parallel antenna array model is introduced at 10GHz demonstrating the effectiveness of different beamforming algorithms, together with preliminary results of a larger array scenario for wireless power transfer over 5.9km to a receiving array in a 5km square map tile.

1 Introduction

The recent interest in Space-based Solar power as a potential solution to the search for reliable, green energy. These solutions are based upon a variety of satellite concepts to generate power from photovoltaic orbital 'farms' and transferring the power to ground based receiving stations wirelessly using microwaves. In order to beam power over long distances, there are broadly three different technologies considered, optical, high frequency microwaves and low frequency microwaves. Of these options microwaves in the frequency range 1-10GHz are considered the optimum tradeoff for space-based solar power (SBSP), as while relatively large apertures are required for efficient transfer, this range offered reduced atmospheric attenuation and improved conversion efficiency [1].

Initial demonstrations of wireless power transfer were carried out by Brown [2], culminating with the Goldstone tests which still hold the record for the highest power transferred wirelessly over a long distance [1]. A range of different solar generation and transmission architectures have been proposed, conventional phased arrays with either mirror redirection to conventional photovoltics or a large stack of photovoltaics spaced away from the transmitter, such as SPS-Alpha and the Sun Tower [3, 4] represent the simplest to model despite their size, as the antenna arrays themselves are planar. An alternative architecture is CASSIOPeiA, which uses a helix structure with omnidirectional antenna elements to allow for consistent beamforming through 360^o in azimuth [5]. Whatever the architecture of interest, SBSP satellites have been proposed with over a billion antenna elements, with diameters on the order of 2km. In order to model the performance of these systems, an efficient, flexible model is required which can predict the near field performance of gigascale antenna arrays.

2 Scalable Electromagnetics

In order to develop a scalable approach to modelling wireless power transfer two aspects were considered. The overall computational approach to modelling gigascale electromagnetics problems were based around a pragmatic assessment of the computation required for kilometer scale antenna arrays. The available open source model (LyceanEM) was capable of handling problem sizes around $1 * 10^7$ rays using a Numba-CUDA accelerated python implementation and modelling at the desired scale would require $1 * 10^{20}$ rays [6]. While such scales will likely always require dedicated high performance computing, a raycasting acceleration approach was required to improve speed at which each path could be checked and calculated. In this work, this acceleration approach will be introduced, together with a development of the Rayleigh-Sommerfeld Diffraction Integral to support near-field wireless power transfer at scale.

2.1 Computational Approach

The original Numba-CUDA Python implementation of the electromagnetic (EM) propagation model used a hybrid GPU/CPU approach, where both raycasting and EM attenuation were GPU, but intermediate filtering steps were performed on the CPU [7] The first CUDA version took this approach and achieved an order of magnitude speed up [8]. The back-and-forth between the CPU and GPU introduced significant latency allowing for a further order of magnitude speed up when all operations were moved to the GPU. By experimenting with further optimizations, such as kernel fusion, vectorized data types, and different data structures, the code saw a further increase in performance on the order of 180 times faster for one of the public facing tutorials.

This increase while impressive is not sufficient for the planned modelling of gigascale electromagnetics problems, despite the efficiency of the Moller algorithm [9]. To solve this the raycasting moved from a brute force ray triangle intersection method, to a tile based acceleration approach. This was loosely based of the the work of Henning and that in the envisaged scenario the majority of the triangles are on the earth which can be taken as a pseudo-plane from the prospective of our SBSP satellite [10, 11]. Before the raycasting happens all triangles are binned into a grid according to there position in this 2D plane. The boundaries of each bin are then used to eliminate all triangles in bins not intercepted by the ray. This approach allows the computational complexity to go from $O(Rays) * O(Triangles)$ to $O(Rays) * O(\sqrt{Triangles})$. While there is a computational overhead generating the tiles, so in scenarios where there are no triangles the brute force CUDA approach is faster, large ray and triangle models such as introduced in Section 3.2 are simply not possible with the brute force approach.

2.2 Electromagnetics

The propagation algorithm selected as part of the SCOPES development is a derivation of the Rayleigh-Sommerfeld Diffraction Integral [12], with changes to support polarimetric (covering all field polarisations) modelling of radio propagation. In order to find the field at observation point p_0, we need to solve the Greens theorem identity for the fully enclosing surface **S**, for which

$$U(p_0) = \int\int_S (U\frac{\partial G}{\partial n} - G\frac{\partial U}{\partial n})ds \tag{1}$$

In order to simplify and solve we can partition into two parts, one representing the aperture of interest S_1, and the remaining enclosing surface S_2 via $S = S_1 + S_2$. The Sommerfeld Radiation condition maintains that as R becomes large the contribution on S_2 tends to zero and can be neglected [12]. Then via the Kirchhoff boundary conditions defining the field outside the aperture $\sum$ in S_1 as zero. Thus the total field at the observation point p_0 can be defined as

$$U(p_0) = \frac{1}{2\pi}\int\int_\Sigma (U\frac{\partial G}{\partial n} - G\frac{\partial U}{\partial n})ds \tag{2}$$

and the first Rayleigh-Sommerfeld solution can be used to find the resultant field at the observation point p_0 due to the aperture $\sum$ as

$$U(p_0) = -\frac{1}{2\pi}\int\int_\Sigma U(p_1)\frac{\partial G}{\partial n}ds \tag{3}$$

For which $U(p_n)$ can be defined via the area ds on the aperture $\sum$ with amplitude A and phase ϕ as $U(p_n) = Ae^{i\phi}$. While G can be defined as the expanding spherical wave from a source at the observation point to p_n as

$$G = \frac{e^{ikr_{01}}}{r_{0,n}} \tag{4}$$

$$\frac{\partial G}{\partial n} = \cos(\vec{n_{p_1}}, \vec{r_{(0,n)}})(ik - \frac{1}{r_{(0,n)}})\frac{e^{ikr_{(0,n)}}}{r_{(0,n)}} \tag{5}$$

This is the lossless simple case, and so for a lossy medium the expression for G and it's partial derivative with respect to n will need to be replaced with

$$E(r) = E_0 e^{\alpha r} e^{i(\beta r + \psi)} \tag{6}$$

Which can then be used to derive the expression given in Equations 7.

$$\frac{\partial G}{\partial n} = (\alpha + i\beta - \frac{1}{r_{(0,n)}})\frac{e^{(\alpha+i\beta)r_{(0,n)}+\psi}}{r_{(0,n)}} \tag{7}$$

These terms allow the prediction of the propagation of a wave from a defined aperture through a lossy medium such as the atmosphere via the specification of appropriate propagation constants, but represents an isotropic solution. A development of this approach allows for the inclusion of polarised field components is the use of the transition matrix $A_{\vec{r}}$ which represents the field components propagating in the direction of ray $\vec{r}_{(0,n)}$, as shown in Equation 8.

$$U(p_0) = -\frac{1}{2\pi}\int\int_\Sigma UA_{\vec{r}_{(0,n)}}(\alpha + i\beta - \frac{1}{r_{(0,n)}})\cos(\vec{n_{p_n}}, \vec{r_{(0,n)}})\frac{e^{(\alpha+i\beta)r_{(0,n)}+\psi}}{r_{(0,n)}}ds \tag{8}$$

2.3 Beamforming

In order to consider wireless power transfer, three different beamforming algorithms were considered for comparative analysis. Wavefront, a conventional farfield beamforming algorithm with flat amplitude weights and phase weights based on the direction of interest. Equiphase, a near-field beamforming algorithm using phase weights based upon the distance of each element from target point, and Equiphase phase weights with Kaiser window function used to generate amplitude weights for increased directivity. Equiphase can be replicated by transmitting a pilot beam from the receiver to the transmitter, and sampling the pilot signal at each element to generate the phase conjugate which can then be used as the phase weight for that element [13, 5].

3 Results

3.1 Small Scale Power Transfer

In order to consider the effects of different beamforming algorithms on overall power transfer efficiency at a convenient model size, a reference case was chosen with identical antenna arrays for the transmitter and receiver at 10GHz. The antenna arrays were each specified as square arrays with an inter-element spacing of 0.4941λ, and 2m square,

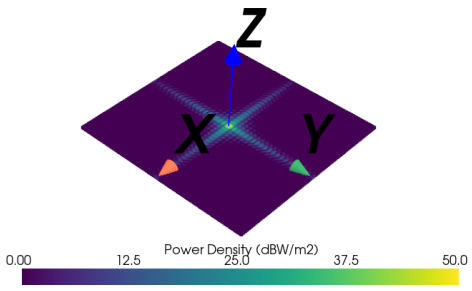

Figure 1. Received Power Density for Equiphase beamforming algorithm at 3m separation

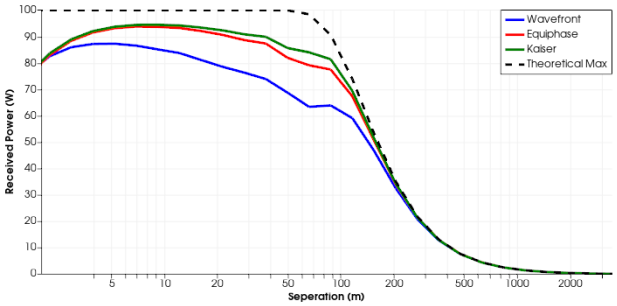

Figure 2. Comparison of power transfer efficiency with Theoretical Maximum for different beamforming algorithms

with 18225 elements in each antenna array. The transmitting antenna elements linearly polarized (aligned with the y axis as shown in Figure 1). The total power transferred with each beamforming algorithm is shown in Figure 2 compared to the theoretical maximum as derived by Goubau [14] for a transmit power of 100W. This is defined in terms of the transmit and receive aperture area, wavelength λ, and separation D, via Equation 9 in order to calculate maximum efficiency Equation 10.

$$\tau = \frac{\sqrt{(A_t A_r)}}{\lambda D} \tag{9}$$

$$\eta = 1 - e^{\tau^2} \tag{10}$$

A range of 50 individual ranges were considered in the model, with a total time per simulation of 130 seconds. Using the Numba accelerated python version.

3.2 Large Scale Power Transfer

The large scale example places a notional antenna array in a rural area in Walton-in-Gordano. This example model uses a digital surface model provided by the National Lidar Program in order to create a populated topographical 5 km grid square [15].

The desired test scenario was to consider a scaled down arrangement based upon the geometry of a geosynchronus

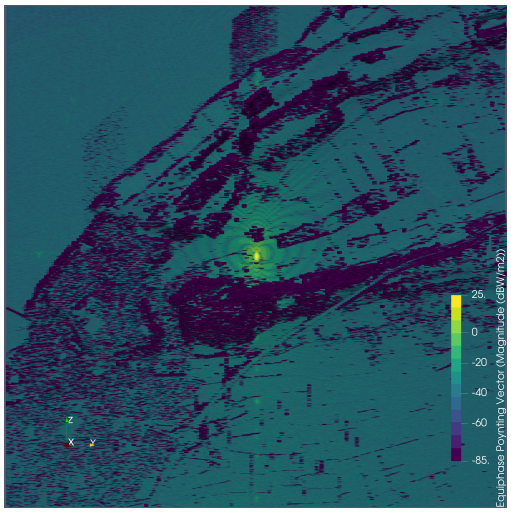

Figure 3. Walton-in-Gordano Large scale model with receiving antenna array placed centrally

satelite, with the range, transmitter and receiver sized for a maximum transfer efficiency of 80%. This was calculated via Equation 10, and set the range at 5.9km.

The transmitting aperture is specified as a circular array with a radius of 17.2135m, with an operating frequency of 2.4GHz, 250,000 elements and an inter-element spacing of 0.5λ. A transmit power density of 240 W/m^2 was selected for the transmitter, resulting in a total transmit power of 223.4kW. The transmitting polarization was circular. The transmitting array was placed 5.9km from the receiver at an elevation angle of 31.2^o, replicating the illumination geometry of a satellite in geosynchronous orbit.

The receiving antenna array was defined as an ellipse with a major radius of 37.32m, a minor radius of 31.94m, and 1 million antenna elements. The receiving array was aligned parallel with the ground, to represent the simplest case for a rectenna array installation. To consider the effects of the power transfer beam on the wider area a sparse set of sample points were defined on the digital surface model with a spacing of 5m for an additional 1,000,000 sample points, which can be seen with the receiving antenna array in Figure 3. The beamforming algorithm used for the figure was the Equiphase method with no amplitude weightings.

Two beamforming algorithms were considered for the large scale model, both the wavefront and equiphase beamforming. The resultant power received at the rectenna array and total transfer efficiency is provided in Table 1. While the array sizes and separation were selected for a maximum transfer efficiency of 80%, this would be for parallel antenna arrays. The receiver's angular offset from the boresight of the transmitter is 59^o. If the antenna array was arranged into subarrays aligned onto the transmitter, this would be significantly higher.

Beamforming Algorithm	Total Power (kW)	Efficiency (%)
Wavefront	73.26	33
Equiphase	80.39	36

Table 1. Received Power and Efficiency for large scale model

4 Conclusions

LyceanEM was originally developed for rapid virtual prototyping of antenna arrays for complex systems in the farfield. The shift of the codebase to the diffraction integral and improvements to the computational efficiency enable it's application to very large antenna arrays and antenna array development. The large scale power transfer model shown in Section 3.2 demonstrates the potential for examining these problems on single GPUs, but in order to handle full scale models future development will be needed to support convenient parallelisation onto multi GPU high performance computing resources. In the future examination of offset feed reflector rectenna arrays could an attractive alternative to flat panel rectenna arrays, and can be expected to offer higher illumination efficiency when properly aligned on the transmitter [13].

5 Acknowledgements

The authors wish to acknowledge the funding from UK Department of Energy Security and Net Zero for supporting the above research work.

6 References

[1] Christopher T. Rodenbeck et al. "Microwave and Millimeter Wave Power Beaming". In: *IEEE Journal of Microwaves* (2021). DOI: 10.1109/jmw.2020.3033992. URL: http://doi.org/10.1109/jmw.2020.3033992.

[2] W. C. Brown. "Experiments in the transportation of energy by microwave beam". In: *IRE International Convention Record* (1964). DOI: 10.1109/irecon.1964.1147324. URL: http://doi.org/10.1109/irecon.1964.1147324.

[3] John C. Mankins, Nobuyuki Kaya, and Massimiliano Vasile. "SPS-ALPHA: The First Practical Solar Power Satellite via Arbitrarily Large Phased Array (A 2011-2012 NIAC Project)". In: *7th International Energy Conversion Engineering Conference* (2012). DOI: 10.2514/6.2012-3978. URL: http://doi.org/10.2514/6.2012-3978.

[4] John C Mankins. "A TECHNICAL OVERVIEW OF THE "SUNTOWER" SOLAR POWER SATELLITE CONCEPT". In: *Acta Astronautica* 50.6 (2002), pp. 369–377. ISSN: 0094-5765. DOI: https://doi.org/10.1016/S0094-5765(01)00167-9. URL: https://www.sciencedirect.com/science/article/pii/S0094576501001679.

[5] Ian Cash. "CASSIOPeiA solar power satellite". In: *2017 IEEE International Conference on Wireless for Space and Extreme Environments (WiSEE)*. 2017, pp. 144–149. DOI: 10.1109/WiSEE.2017.8124908.

[6] Timothy G. Pelham. "LyceanEM: A python package for virtual prototyping of antenna arrays, time and frequency domain channel modelling". In: *Journal of Open Source Software* 8.86 (2023), p. 5234. DOI: 10.21105/joss.05234. URL: https://doi.org/10.21105/joss.05234.

[7] Siu Kwan Lam, Antoine Pitrou, and Stanley Seibert. "Numba: A llvm-based python jit compiler". In: *Proceedings of the Second Workshop on the LLVM Compiler Infrastructure in HPC*. 2015, pp. 1–6.

[8] NVIDIA, Péter Vingelmann, and Frank H.P. Fitzek. *CUDA, release: 10.2.89*. 2020. URL: https://developer.nvidia.com/cuda-toolkit.

[9] Tomas Möller and Ben Trumbore. "Fast, Minimum Storage Ray-Triangle Intersection". In: *Journal of Graphics Tools* (1997). DOI: 10.1080/10867651.1997.10487468. URL: http://doi.org/10.1080/10867651.1997.10487468.

[10] Christian Henning and Peter Stephenson. "Accelerating the ray tracing of height fields". In: GRAPHITE04 (June 2004), pp. 254–258. DOI: http://dx.doi.org/10.1145/988834.988878.

[11] Amy L. Williams et al. "An Efficient and Robust Ray-Box Intersection Algorithm". In: *Journal of Graphics Tools* (2005). DOI: 10.1080/2151237x.2005.10129188. URL: http://doi.org/10.1080/2151237x.2005.10129188.

[12] Joseph W. Goodman. *Introduction to Fourier optics*. Page 44. Roberts Co. Publishers, 2004, p. 44. ISBN: 9780974707723.

[13] Timothy Pelham et al. "An Overview of Gigascale Antenna Arrays and Electromagnetics for Space Based Solar Power". In: *2024 18th European Conference on Antennas and Propagation (EuCAP)*. 2024, pp. 1–4. DOI: 10.23919/EuCAP60739.2024.10501466.

[14] G. Goubau and F. Schwering. "On the guided propagation of electromagnetic wave beams". In: *IRE Transactions on Antennas and Propagation* 9.3 (May 1961), pp. 248–256. DOI: 10.1109/tap.1961.1144999. URL: http://doi.org/https://doi.org/10.1109/tap.1961.1144999.

[15] Environment Agency. *National LIDAR Programme*. 2019. URL: https://www.data.gov.uk/dataset/f0db0249-f17b-4036-9e65-309148c97ce4/national-lidar-programme#licence-info.